J Mater Sci (2011) 46:316–326
DOI 10.1007/s10853-010-4812-x

Structure, conductivity and redox stability of solid solution $Ce_{1-x}Ca_xVO_4$ ($0 \leq x \leq 0.4125$)

Christophe T. G. Petit · Rong Lan · Peter I. Cowin · Arno Kraft · Shanwen Tao

Received: 9 June 2010 / Accepted: 29 July 2010 / Published online: 12 August 2010

Abstract A-site-substituted cerium orthovanadates, $Ce_{1-x}Ca_xVO_4$, were synthesised by solid-state reactions. At room temperature, the solid solution limit in $Ce_{1-x}Ca_xVO_4$ series is at $x = 0.4125$. The crystal structure was analysed by X-ray diffraction and it exhibits a tetragonal zircon structure of space group $I4_1/amd$ with $a = 7.4004$ (1) and $c = 6.4983$ (6) Å for $CeVO_4$. The UV–Visible absorption spectra indicated that the compounds have band gaps at room temperature in the range of 4.2–4.5 eV. Conductivity measurements were performed for the first time up to the calcium solid solution limit in both air and dry 5% H_2/Ar with conductivity values at 600 °C ranging from 0.3 to 20 mS cm^{-1} in air to 3 to 30 mS cm^{-1} in reducing atmosphere. In general, the conductivity of Ca-doped $CeVO_4$ is higher in air but lower in a reducing atmosphere comparing to pure $CeVO_4$. The H_2/air electrochemical cell measurement indicates that the conduction of sample $Ce_{0.7}Ca_{0.3}VO_4$ is electronic dominant. Samples $Ce_{0.9}Ca_{0.1}VO_4$ and $Ce_{0.8}Ca_{0.2}VO_4$ are redox stable at a temperature below 600 °C although the conductivity is not high enough to be used as an electrode for solid oxide fuel cells.

Introduction

Rare earth orthovanadates ($REVO_4$) have been intensively studied in the last two decades, in particular lanthanoid orthovanadates ($LnVO_4$) due to the interesting physical properties exhibited by those compounds (luminescence, Jahn–Teller phase transitions, et cetera). First studied in the 1950s as part of investigations to determine precise crystal structures [1], atomic arrangements in chemical series and ionic radius of crystals comprising heavy metals [2], $REVO_4$ exhibit an ABO_4 structure, where two crystallisation types are observed: tetragonal zircon [3] and monoclinic monazite [4]. More generally, larger lanthanoid ions prefer the monazite type, while smaller lanthanoids crystallise in the zircon type [5]. Interestingly, cerium (III) orthovanadate ($CeVO_4$), which according to phase diagrams is located at the boundary of zircon and monazite types, exhibits three polymorphic forms with the pseudo-octahedral looking-like structure of tetragonal scheelite in addition to the zircon (Z) and monazite (M) type forms. Structurally speaking, $CeVO_4$-(Z) is composed of tetragonal bisphenohedra of VO_4, edge-linked to CeO_8 triangular dodecahedra along the *c*-crystal axis, and VO_4 tetrahedra corner-linked with CeO_8 dodecahedra along the *a*- and *b*-crystal axes. Additionally, channels along the *c*-crystal axis—Fig. 1—[6], octagonal in shape, allow the insertion of ions and the use of cerium vanadates in catalytic processes [7]. One study by Mahapatra et al. [8] focussed on the use of doped cerium orthovanadates in photocatalysis and photo-oxidation of dyes and organics like cyclohexane and benzene.

In the first studies of heavy metal orthovanadates ($HMVO_4$), researchers started to focus on crystal structures and group theory, looking for answers to explain the specific characteristics obtained when heavy metals and less generally RE elements of the f-block were mixed with orthovanadates. Based on a synthetic protocol previously established [9], Milligan and Vernon [1] reported structural studies on a group of 15 $HMVO_4$ among which 13 were lanthanoids. They demonstrated using X-ray diffraction that the crystals had crystallised in body-centred tetragonal systems, space group $I4_1$/amd.

C. T. G. Petit · R. Lan · P. I. Cowin · A. Kraft · S. Tao (✉)
Department of Chemistry, Heriot-Watt University, Edinburgh EH14 4AS, UK
e-mail: S.Tao@hw.ac.uk

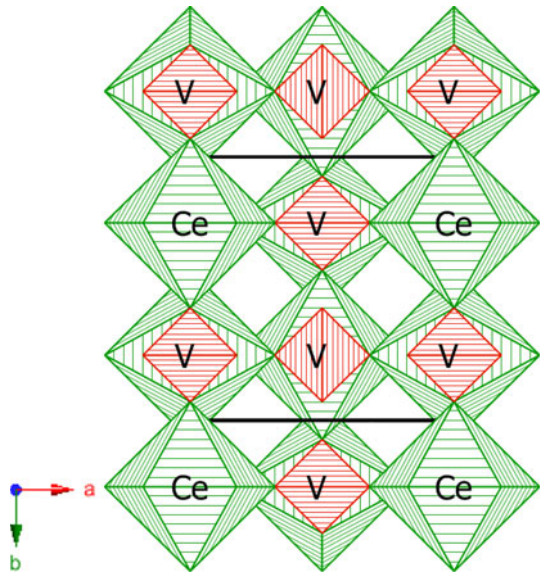

Fig. 1 Structural model of $CeVO_4$-(Z) showing the channels along the *c*-crystal axis

In the last decade or so, studies on members of the RE group were forsaken in bulk and attention was put onto specific orthovanadates (cerium and lanthanum essentially). The first study on the electrical and thermal behaviours of $CeVO_4$ was reported by Rao and Palanna [10]. Rao and Palanna used the conventional solid-state ceramic technique to synthesise $CeVO_4$. Whereas $CeVO_4$ in itself is an insulator whether in pure or stoichiometric composition, a *p*-type semiconductive behaviour between room temperature and 800 °C was observed. An explanation given to account for the *p*-type conduction in the lattice was that among the Ce^{3+} ions, coexisted a few number of Ce^{4+} ions and that therefore the conduction was occurring via thermally activated motions of ions on equivalent sites.

Recently, doped $REVO_4$ have also being studied, particularly lanthanide and cerium orthovanadates doped with other RE [11] or with elements like calcium [12–16], iron [17, 18], bismuth [12, 13] or strontium [12–16] notably.

Firstly reported in the twenty-first century by Watanabe [12] with the study of highly conductive oxides, rapidly followed by the comparative study of Hirata and Watanabe [13] on calcium- and bismuth-doped cerium orthovanadates, $RE_{1-x}A_xVO_4$ species have attracted growing interest in the past years for their spectacular physical properties, including an excellent conductivity. Tsipis et al. [16] published in 2002 a study on the transport and physicochemical properties of A-substituted $CeVO_4$ with calcium and strontium, namely $Ce_{1-x}A_xVO_{4\pm\delta}$ (A = Ca, Sr; x = 0–0.2). Samples were synthesised following a standard ceramic technique and XRD was used for verification of single zircon-type phase formation. The thermal expansions of the $Ce_{1-x}A_xVO_{4\pm\delta}$ were found to be almost linear for both doping agents in a range from 400 to 800 K. The study also revealed that doping with calcium considerably enlarged the zircon phase stability domain of $Ce_{1-x}A_xVO_4$ and also considerably enhanced the specific stability of zircon-type $Ce_{1-x}A_xVO_4$ at reduced oxygen pressures. A paper published a year after by the same group [15] focussed on the oxygen ionic conductivity of $Ce_{1-x}A_xVO_{4+\delta}$ (A = Ca, Sr; x = 0–0.2). Referring to the paper by Watanabe [12] where $Ce_{0.8}Ca_{0.2}VO_4$ and $Ce_{0.9}Sr_{0.1}VO_4$ were found to give the maximum conductivity in air, ionic conductivity and stability measurements were performed on oxygen in $Ce_{1-x}A_xVO_{4+\delta}$. It was found that $Ce_{1-x}A_xVO_{4+\delta}$-(Z) was stable in air up to 1300 K showing no phase transitions, and that the oxygen ionic conductivity was actually essentially independent of the concentration of the A-site dopant: in opposition with *p*-type electronic conduction, determined by the dopant concentration.

While studied at low doping factor (up to 0.2), some aspects of calcium-doped cerium orthovanadates have yet still to be fully explored. As mentioned by Tsipis et al. [16], the doping of cerium orthovanadates with calcium increases an already highly conductive oxide. This study therefore aims to investigate the phase (solid solution limit) and conductive behaviour in $Ce_{1-x}Ca_xVO_4$ at higher doping level up to the solid solution limit. The conductivity in a reducing atmosphere was also investigated to evaluate the potential use as redox stable anode for intermediate temperature solid oxide fuel cells.

Experimental

Materials

CeO_2 (Alfa-Aesar, 99.9% REO), V_2O_5 (Aldrich, 99.6+% metals basis) and $CaCO_3$ (Alfa-Aesar, ACS 99.0% min) for the solid-state synthesis method were used as received.

Preparation

Pure, non-doped cerium orthovanadates were synthesised by a solid-state method using CeO_2 and V_2O_5 as cerium and vanadium sources, respectively. For the solid-state syntheses, stoichiometric amount of the respective oxides were fired at 800 °C at a heating rate of 5 °C min^{-1} for a dwelling time of 50 h. $Ce_{1-x}Ca_xVO_4$ compounds were synthesised by a solid-state method using CeO_2, V_2O_5 and $CaCO_3$ as cerium, vanadium and calcium sources, respectively. For the Ca-doping syntheses, stoichiometric amount of the respective oxides was fired at 850 °C or at 900 °C—depending on the doping factor—at a heating rate of

5 °C min^{-1} and maintained for 66 h. x varied from 0.1 to 0.7 and a pure phase was obtained with $x \leq 0.4125$.

Characterisation

UV–vis absorption

The band gaps at room temperature of all synthesised compounds were determined graphically from spectra obtained using a UV–visible spectrophotometer (Shimadzu UV-2550) operating with UVProbe® software.

X-ray powder diffraction

X-ray data were collected on a Bruker-AXS (D8 Advance) diffractometer, controlled by DIFFRACT$^{plus\ TM}$, in the Bragg–Brentano reflection geometry with a Ni-filtered Cu Kα source (1.5405 Å), fitted with a LynxEye^{TM} detector. Absolute scans in the 2θ range of 5–85° with step size of 0.009° and time step of 61.6 (123.2 s for sample at $x = 0.4125$) were used during data collection.

Scanning electron microscopy

SEM pictures were taken with the use of a Quanta 3D FEG scanning electron microscope (FEI Company) with charges of 10 kV and 10 pA.

Conductivity

Total conductivity measurements were carried out using a computer-controlled Solartron Analytical® SI 1260 impedance/gain phase analyser over a frequency range of 1 MHz to 0.01 Hz and a temperature range of 700 °C to room temperature (~25 °C) and impedance data were recorded with the Solartron Impedance Measurement software, SMaRT^{TM}. Sample powders were pressed into pellets and sintered at temperatures depending on the sample themselves for 12 h (650 °C for $CeVO_4$, 850 °C for Ca-doped compounds). The relative densities for samples with $x = 0$, 0.1, 0.2, 0.3, and 0.4 were 85, 82, 80, 86, and 80%, respectively. Pellets were coated with silver paste for measurements in air and with platinum paste for measurements in a reduced atmosphere of 5% H_2/Ar dried through a solution of H_2SO_4 at 98%. Pellets coated with silver were directly fitted into the measuring apparatus while platinum coated samples were fired at 850 °C at a rate of 5 °C min^{-1}, dwelled for 2 h and then cooled down to room temperature before being used for pseudo 4-probe ac impedance measurements. Measurements in air were carried out on heating and those in reduced atmosphere on cooling after stabilisation was achieved.

H_2/air electrochemical cell measurement

The pellet of sample $Ce_{0.7}Ca_{0.3}VO_4$ was coated a layer of platinum electrode on both side then fired at 850 °C for 1 h in air before the electrochemical cell measurements. Dry 5% H_2 in Argon was passed through 98% H_2SO_4 before being feed at the anode side of the cell with the other side open to air. Open circuit voltage (OCV) of the electrochemical cell was measured with use of a Solartron 1287 electrochemical interface controlled by CorrWare/CorrView® for automatic data collection.

Results and discussion

Crystal structure

Single-phase powders of $Ce_{1-x}Ca_xVO_4$ were obtained up to $x = 0.4125$ (Fig. 2); for higher x values, a second phase corresponding to $Ca_2V_2O_7$ was formed indicating that the solid solution limit in $Ce_{1-x}Ca_xVO_4$ series is at about $x = 0.4125$. Rietveld refinements were carried out with both structural and profile parameters being varied. Initial structural and spatial parameters for the zircon structure were used as mentioned in the literature [5]. Wyckoff sites assigned to Ce and Ca, V and O were 4*a*, 4*b* and 16 *h*, respectively. Vanadium and oxygen were always considered—during the refinement processes—with full occupancies, whereas cerium and calcium occupancies were varied in accordance with the stoichiometry. It is difficult to refine the oxygen occupancy because XRD is not sensitive to light atoms such as oxygen. Profile refinements were performed using GSAS [19]. The experimental and calculated profile for $Ce_{0.8}Ca_{0.2}VO_4$ is shown in Fig. 3. The refined parameters are listed in Table 1 for $Ce_{1-x}Ca_xVO_4$ and the average bond lengths in Table 2.

The tetragonal system exhibited by $CeVO_4$ with a zircon-type structure was found to be also representative of the calcium doping level. Increasing the dopant level up to the boundary of doping decreases the size of the primary unit cell as shown by the decreasing values of the lattice parameters (Fig. 4). As the ionic radius of Ca^{2+} (1.12 Å) is smaller than that for Ce^{3+} (1.143 Å) at coordination number of eight [20], replacing Ce^{3+} ions by Ca^{2+} ions should not cause any significant lattice contraction if the charge of the cerium ions remained unchanged. However, continuous lattice contraction was observed when more calcium was introduced in the lattice. This reduction in size may be due to the formation or the transformation of some components of the lattice into smaller counterparts; namely the formation of Ce^{4+} to balance the charge animosity introduced by the doping with Ca^{2+} because the ionic size of Ce^{4+} ions is only 0.97 Å when eight-coordinated [20].

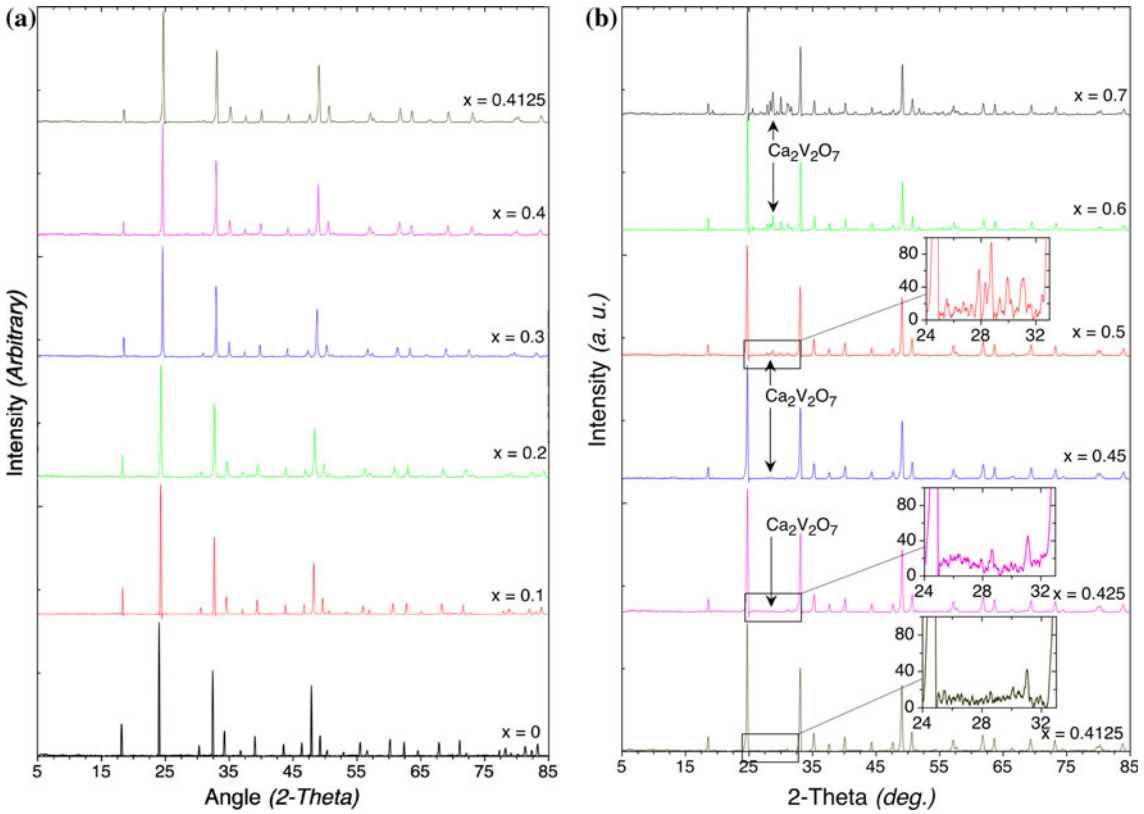

Fig. 2 X-ray diffraction patterns of **a** $Ce_{1-x}Ca_xVO_4$ with $0 \leq x \leq 0.4125$ and **b** $Ce_{1-x}Ca_xVO_4$ with $0.4125 \leq x \leq 0.7$

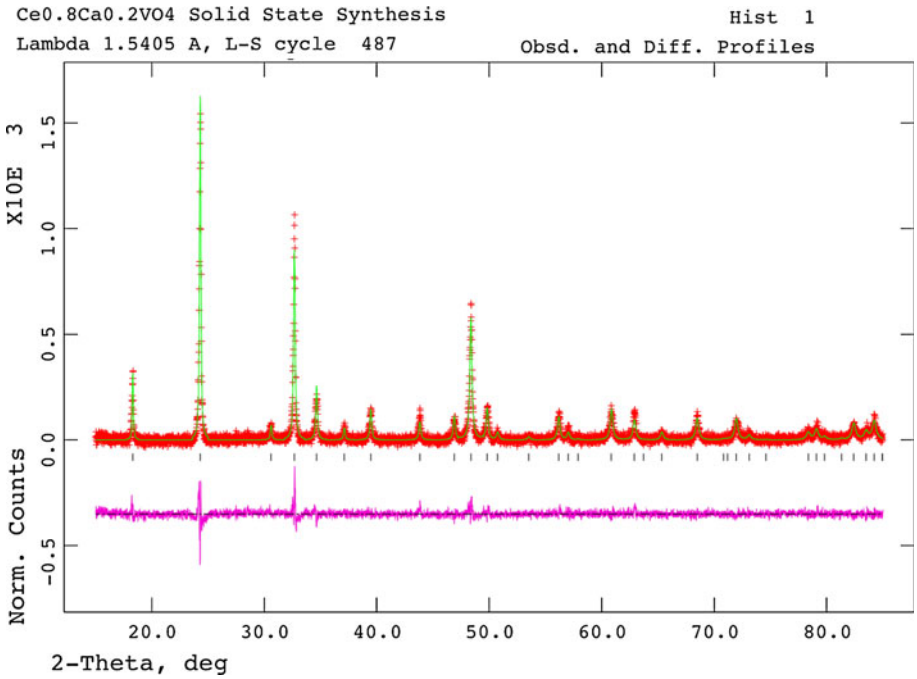

Fig. 3 Representation of an experimental (*crossed*) and calculated (*solid line*) X-ray diffraction profiles for $Ce_{0.8}Ca_{0.2}VO_4$. The difference profile is shown at the bottom of the profile

The charge compensation in $Ce_{1-x}Ca_xVO_4$ could be in two ways: (a) the formation of oxygen-deficient oxides with the charge for cerium ions remaining 3+, which might lead to lattice expansion due to the formation of oxygen vacancies which is inconsistent with the observed lattice contraction; (b) some Ce^{3+} ions are converted to Ce^{4+} ions with the oxygen content remaining stoichiometric or with an oxygen excess. It has been reported that the results on

Table 1 Crystallographic refinement parameters of $Ce_{1-x}Ca_xVO_4$ with $0 \leq x \leq 0.4125$

Crystallographic parameter	$CeVO_4$	$Ce_{0.9}Ca_{0.1}VO_4$	$Ce_{0.8}Ca_{0.2}VO_4$	$Ce_{0.7}Ca_{0.3}VO_4$	$Ce_{0.6}Ca_{0.4}VO_4$	$Ce_{0.5875}Ca_{0.4125}VO_4$
r Ln^{3+} (VIII) (Å)	1.143	1.143	1.143	1.143	1.143	1.143
λ (Å)	1.5405	1.5405	1.5405	1.5405	1.5405	1.5405
Crystal system	Tetragonal	Tetragonal	Tetragonal	Tetragonal	Tetragonal	Tetragonal
Space group	$I4_1/amd$	$I4_1/amd$	$I4_1/amd$	$I4_1/amd$	$I4_1/amd$	$I4_1/amd$
a (Å)	7.4004 (1)	7.3706 (1)	7.3145 (1)	7.2483 (3)	7.2314 (2)	7.2150 (1)
c (Å)	6.4983 (6)	6.4879 (1)	6.4525 (2)	6.4129 (3)	6.4084 (3)	6.4027 (2)
V (Å^3)	355.88 (5)	352.45 (2)	345.22 (1)	336.91 (4)	335.11 (4)	333.30 (3)
ρ_{calc} (g cm^{-3})	4.7601	4.6179	4.5222	4.4365	4.2621	4.2604
Rp (%)	7.88	8.15	7.78	8.89	9.27	6.80
wRp (%)	10.00	10.44	9.74	12.94	12.06	9.01
χ^2	1.463	1.722	1.343	2.081	1.913	1.870

Table 2 Average bond lengths, fraction of Ce^{4+} ions and oxygen hyperstoichiometry in $Ce_{1-x}Ca_xVO_4$ with $0 \leq x \leq 0.412$

	$x = 0$	$x = 0.2$	$x = 0.3$	$x = 0.4$	$x = 0.4125$
Ce–O (Å)	2.4839	2.4595	2.4401	2.4360	2.4318
V–O (Å)	1.7115	1.6949	1.6815	1.6788	1.6759
y_{sp} (%)	5.26 (1)	20.84 (2)	37.98 (4)	46.05 (5)	50.88 (3)
y_o (%)	5.26 (2)	16.67 (2)	26.59 (3)	27.63 (1)	29.89 (3)
δ	0.03 (4)	0.08 (2)	0.13 (1)	0.14 (4)	0.15 (3)

The Ce–O bond lengths were averaged between Ce–O1 and Ce–O2 interatomic distances

structure and electrical properties of Ca-doped $CeVO_4$ suggest moderate oxygen excess in the lattice, leading to an interstitial mechanism [15]. Therefore, it is likely that an oxygen excess solid solution was formed when doped with calcium. The general formula of the compounds can thus be written as $(Ce^{3+}_{1-y}Ce^{4+}_y)_{1-x}Ca_xVO_{4+\delta}$.

Using the same method as in described in our previous report [21], the fraction of Ce^{4+} ions present in each compound can be estimated. In this case, the reduction in volume size and therefore also in the lattice parameters also indicates that the proportion of Ce^{4+} ions present in the structure is increasing linearly from $x = 0.1$ to $x = 0.3$, since from $x = 0.3$ to $x = 0.4125$ changes are in comparison practically negligible. This points out the fact that—as indicated in Table 2 with y_{sp} the fraction of Ce^{4+} ions occupying Ce-site within the structure that are actually occupied by cerium atoms and y_o the overall fraction of Ce^{4+} ions contained within each compound considering the total number of Ce-sites, even if some are in fact occupied by calcium atoms—a limit amount of Ce^{4+} ions able to coexist with Ce^{3+} ions must exist and is achieved before reaching the dopant level limit [21]. Values for the hyperstoichiometry of oxygen range from +0.03 to +0.15 indicate the presence of hyperstoichiometric anions within the lattice.

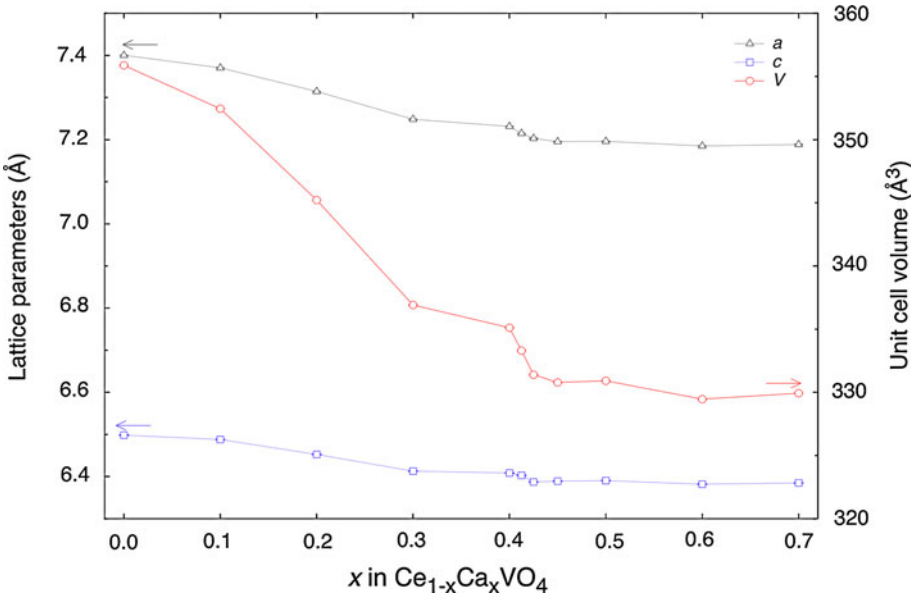

Fig. 4 Lattice parameters and volume reduction in $Ce_{1-x}Ca_xVO_4$ with $0 \leq x \leq 0.7$

Table 3 Band gap energies of $Ce_{1-x}Ca_xVO_4$ with $0 \leq x \leq 0.4125$

	Band gap energy (eV)
$CeVO_4$	4.435 (2)
$Ce_{0.9}Ca_{0.1}VO_4$	4.495 (1)
$Ce_{0.8}Ca_{0.2}VO_4$	4.440 (3)
$Ce_{0.7}Ca_{0.3}VO_4$	4.490 (4)
$Ce_{0.6}Ca_{0.4}VO_4$	4.525 (1)
$Ce_{0.5875}Ca_{0.4125}VO_4$	4.520 (3)

Concerning band gap energies, values were determined following the same procedure as in [21]. The values obtained—tabulated in Table 3 and extracted from the spectra in Fig. 5—show that at room temperature, $Ce_{1-x}Ca_xVO_4$ with $0 \leq x \leq 0.4125$ compounds are insulators, as expected.

SEM pictures were captured as physical evidence of the product's crystalline state. Referring to Fig. 6, $Ce_{0.8}Ca_{0.2}VO_4$ is shown with different magnifications and it can be seen that particles are plain and well sintered with some voids and channels.

Conductivity

Conductivity measurements were carried out in air and in reducing atmosphere of 5% H_2/Ar. Logarithmic plots of conductivity times temperature against inverse temperature were constructed and are shown in Figs. 7 and 8 for air and reduced atmosphere, respectively. Conductivity variations from air to reduced atmosphere at 600 °C are shown in Fig. 9.

Plotted as Arrhenius type plots, activation energies can be extracted from the slope of each series of points, while the Arrhenius constant A can be determined from the intercept values. Those results are shown in Table 4. It was observed, as shown in Fig. 7a, that the doping of $CeVO_4$ with calcium did improve the conductivity of the compounds in comparison with the non-doped sample independently of the temperature.

Samples with $0.2 \leq x \leq 0.4$ did reach a maximum conductivity at 500–550 °C before decreasing slightly up to 700 °C. Variations of conductivity values within the doped compounds were found to be very small and the conductivity improvement therefore seems independent of the dopant level (Fig. 7b).

The introduction of Ca^{2+} results in smaller lattice parameters but the measured band gaps of Ca-doped $CeVO_4$ were similar to that of pure $CeVO_4$ (Table 3). Therefore, the electronic conductivity in air should not be significantly affected. On the other hand, more Ce^{4+} ions will appear in the lattice from charge compensation at higher doping level (Table 2). The higher conductivity of the doped samples in air is likely to be related to the improved oxygen ion conduction due to the increase of charge carriers as oxygen interstitials. Considering standard deviation, the excess oxygen (δ value) in samples with $0.2 \leq x \leq 0.4$ is at a similar level (Table 2) therefore the conductivity in air of these samples are comparable (Fig. 7b).

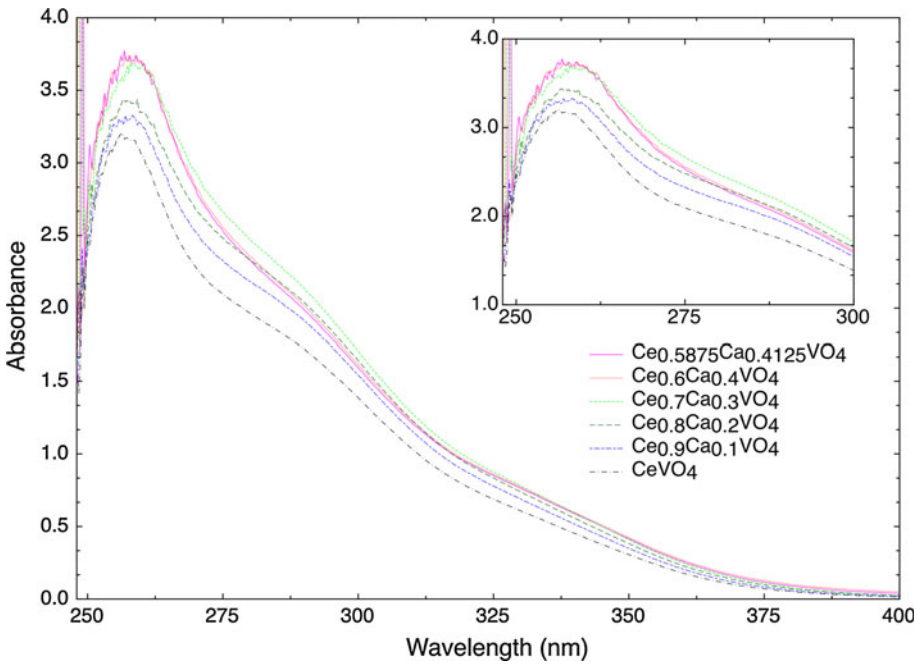

Fig. 5 UV–Vis absorbance spectra of $Ce_{1-x}Ca_xVO_4$ with $0 \leq x \leq 0.4125$

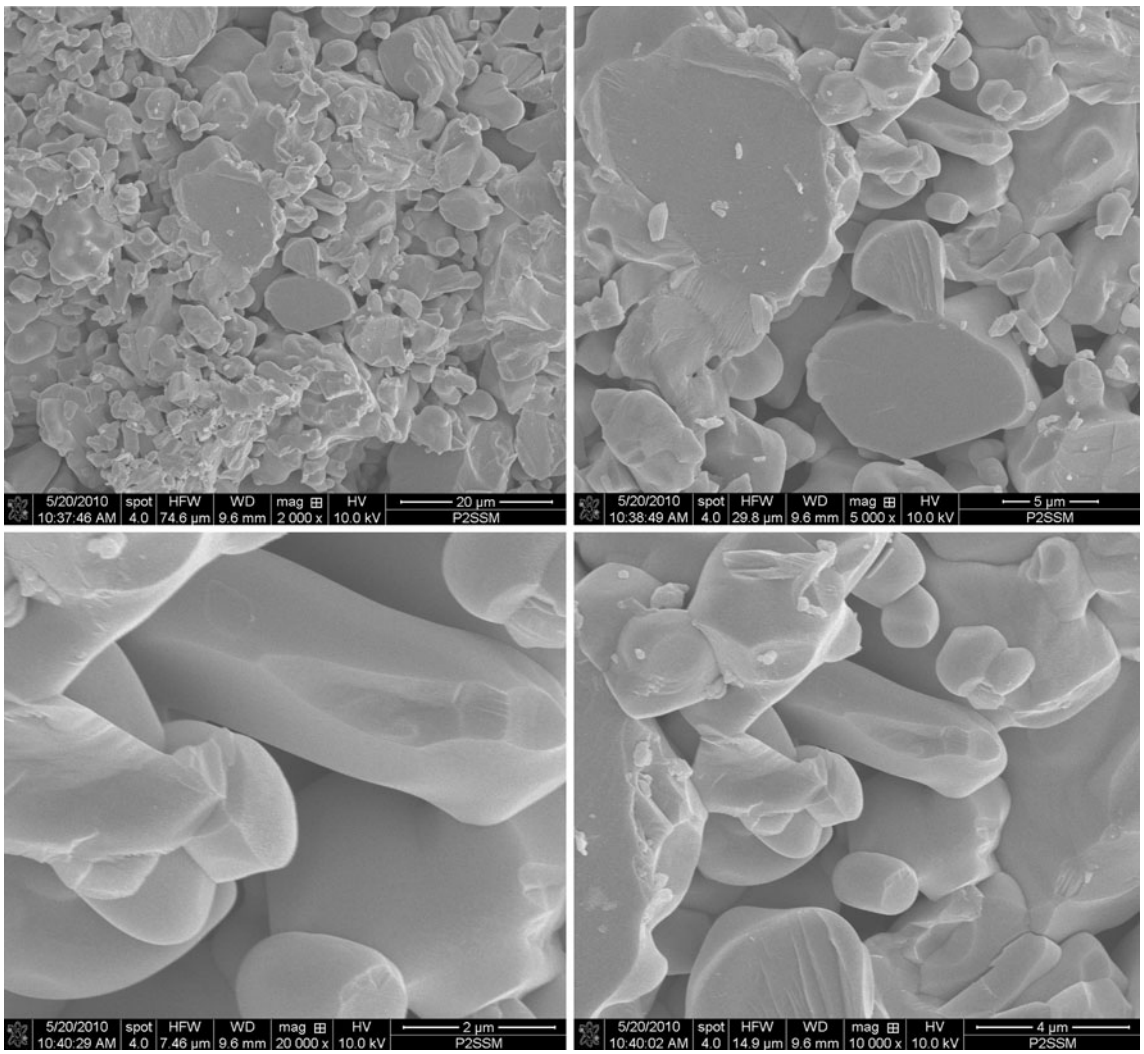

Fig. 6 SEM images of $Ce_{0.8}Ca_{0.2}VO_4$ at magnification ×2000, ×5000, ×10000 and ×20000 clockwise from *top left*

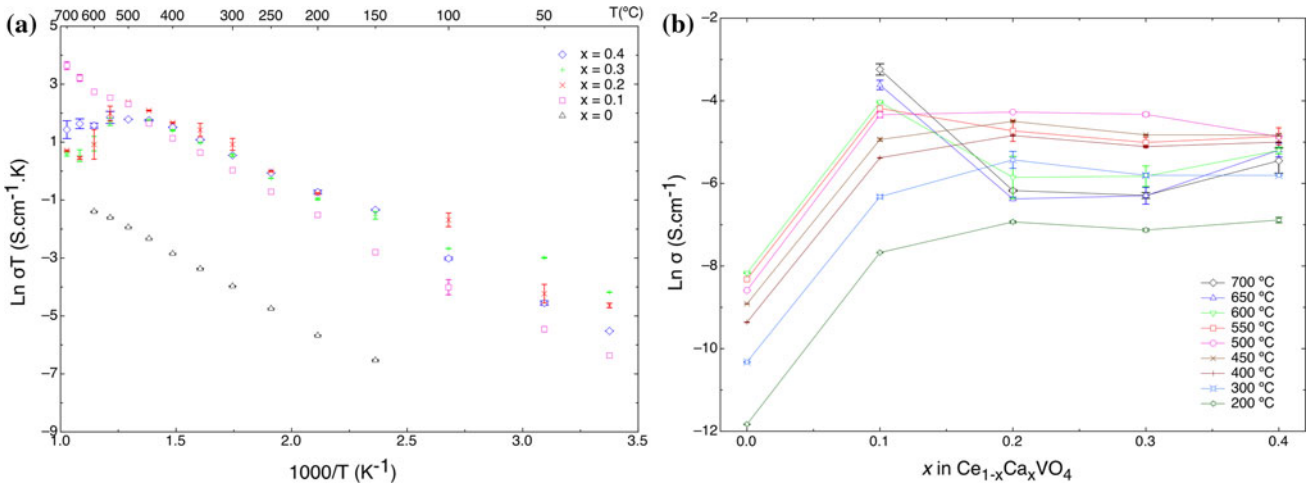

Fig. 7 **a** Arrhenius plots of the conductivity in air of $Ce_{1-x}Ca_xVO_4$ with $0 \leq x \leq 0.4$. **b** Conductivity in air as a function of x in $Ce_{1-x}Ca_xVO_4$ with $0 \leq x \leq 0.4$

$Ce_{1-x}Ca_xVO_4$ compounds with $0 \leq x \leq 0.4$ were found to be stable in air up to the measured temperature of 700 °C, exhibiting a metallic behaviour at 600 °C (Fig. 8). It is likely that a change in the conduction mechanism from a semiconductor to a metal is occurring between 500 and 600 °C, which could be related to the loss of excess oxygen at high temperatures. Activation energies for samples in air were found to be very similar while still lower for doped species when compared to $CeVO_4$. Those variations in activation energies are linked to an increased capability of electron movement allowed by the reduction in size of the lattice parameters created as a consequence of the doping. In our experiments, the conductivities of $CeVO_4$, $Ce_{0.9}Ca_{0.1}VO_4$ and $Ce_{0.8}Ca_{0.2}VO_4$ in air are 2.8×10^{-4}, 2.0×10^{-2} and 3.0×10^{-3} S cm^{-1}, respectively at 600 °C which are lower than those reported by Tsipis et al. [16] namely 2.0×10^{-2}, 1.5×10^{-1} and 2.5×10^{-1} S cm^{-1} for the same considered samples, respectively, under the same conditions. However, the apparent conduction activation energy for $CeVO_4$ and $Ce_{0.9}Ca_{0.1}VO_4$ of 36.3 ± 0.3 and 35.6 ± 0.5 kJ mol^{-1}, respectively (Table 4) is very close to the reported 37.9 ± 0.8 and 35.2 ± 0.6 kJ mol^{-1} [16] although the apparent conduction activation energy for $Ce_{0.8}Ca_{0.2}VO_4$ (28.4 ± 2.3 kJ mol^{-1}) is slightly smaller to the 34.6 ± 0.7 kJ mol^{-1} [16]. The difference may be mainly related to the various measurement methods used. In our experiments, pseudo 4-probe ac impedance spectroscopy was used while 4-probe dc technique was used by Tsipis [16].

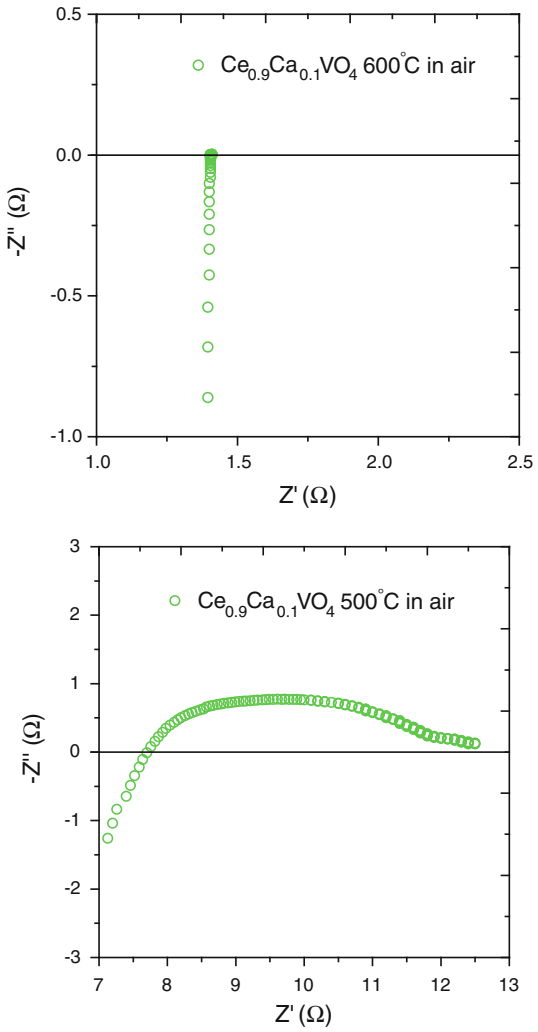

Fig. 8 Conductivity measurement plots of $Ce_{0.9}Ca_{0.1}VO_4$ at 600 and 500 °C in air

Considering measurements in dry 5% H_2/Ar, it can be observed in Fig. 9a that the general conductivity of doped $CeVO_4$ compounds were similar or slightly lowered (except for sample $Ce_{0.7}Ca_{0.3}VO_4$ which was increased); ranging from 2 to 15 mS cm^{-1} at reduced oxygen pressure when compared to 3 to 20 mS cm^{-1} in air. This behaviour is not reproduced with $CeVO_4$ whose maximum conductivity jumps from 0.3 mS cm^{-1} at 600 °C in air to 30 mS cm^{-1} at 600 °C under reduced atmosphere. While the dopant concentration did not influence large conductivity variations in air, it can be seen that the matter is singularly different in reducing atmosphere. Indeed, while all Ca-doped species were more conductive than $CeVO_4$ in air along the whole range of temperatures, only sample $Ce_{0.7}Ca_{0.3}VO_4$ is more conductive than $CeVO_4$ at high temperatures in reduced atmosphere (Fig. 9b). This behaviour can be explained by the oxygen partial pressure dependency of the total conductivity of these compounds introduced with the *p*-type semi-conductive character; as indicated for $CeNbO_4$ by Tsipis et al. [22] namely that the total conductivity of $CeNbO_4$—structurally similar to $CeVO_4$—decreases consequently when the oxygen partial pressure is very low at high temperatures. It should be noted that the measured conductivity of sample $Ce_{0.7}Ca_{0.3}VO_4$ in 5% H_2/Ar is slightly higher than that for sample $CeVO_4$ (Fig. 9b) which could be related the higher relative density (86%) as mentioned above therefore it was not fully reduced even after exposing in 5% H_2/Ar at 600 °C for 12 h (Fig. 10). The decrease in conductivity in 5% H_2/Ar at 600 °C (Fig. 9) is related to the loss of excess oxygen. However, the total conductivity of samples $CeVO_4$ and $Ce_{0.7}Ca_{0.3}VO_4$ did not decrease during the measured 12 h, this could be due to the higher relative densities of these two samples causing slow reduction. At 600 °C, the conductivities of samples $CeVO_4$ and $Ce_{0.7}Ca_{0.3}VO_4$ do not exhibit obvious change against time (Fig. 10) with a decrease in conductivity observed in our samples. This could be explained if these two samples have either significant ionic conduction or if the kinetic process to reach equilibrium for reduction is very fast or very slow. An electrochemical cell was constructed to verify the observed phenomena. OCV curve is shown in Fig. 11 after 10 h (a) and 18 h (b) of exposure to dry 5%

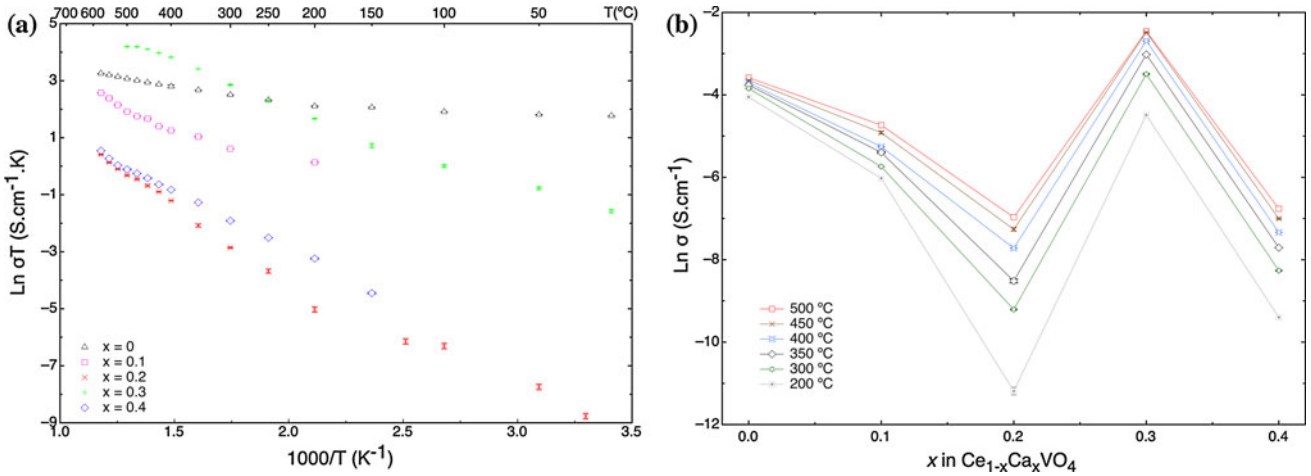

Fig. 9 **a** Arrhenius plots of the conductivity in dry 5% H_2/Ar of $Ce_{1-x}Ca_xVO_4$ with $0 \leq x \leq 0.4$. **b** Conductivity in dry 5% H_2/Ar as a function of x in $Ce_{1-x}Ca_xVO_4$ with $0 \leq x \leq 0.4$

Table 4 Arrhenius constants and activation energies of $Ce_{1-x}Ca_xVO_4$ with $0 \leq x \leq 0.4125$

	$CeVO_4$	$Ce_{0.9}Ca_{0.1}VO_4$	$Ce_{0.8}Ca_{0.2}VO_4$	$Ce_{0.7}Ca_{0.3}VO_4$	$Ce_{0.6}Ca_{0.4}VO_4$
Air					
E_a (kJ mol^{-1})	36.3 ± 0.3	35.6 ± 0.5	28.4 ± 2.3	25.0 ± 0.8	30.2 ± 5.1
A (S K cm^{-1})	38.4 ± 1.1	2119.6 ± 1.1	891.4 ± 1.3	325.4 ± 1.2	932.7 ± 1.1
Dry 5% H_2/Ar					
High temp.					
E_a (kJ mol^{-1})	10.6 ± 0.2	37.6 ± 1.6	47.5 ± 0.6	27.8 ± 0.5	33.5 ± 0.3
A (S K cm^{-1})	112.3 ± 1.0	2562.9 ± 1.3	1279.5 ± 1.1	6001.7 ± 1.1	174.7 ± 1.1
Low temp.					
E_a (kJ mol^{-1})	2.3 ± 0.2	15.5 ± 0.9	25.0 ± 1.8	18.0 ± 0.6	NA
A (S K cm^{-1})	14.8 ± 1.1	55.1 ± 1.2	4.2 ± 1.8	345.8 ± 1.2	NA
Temp. border (°C)	575	575	575	575	NA

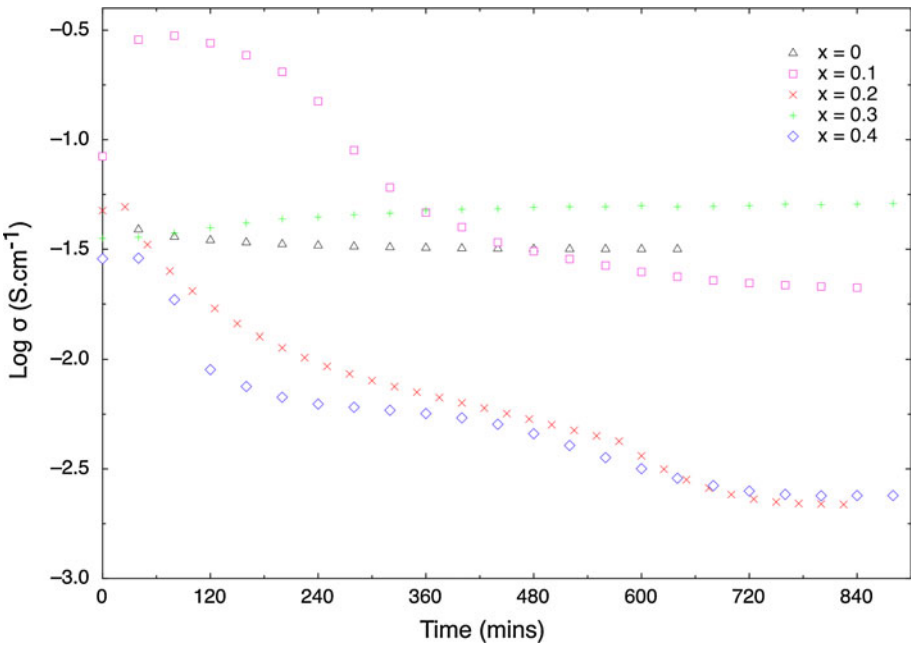

Fig. 10 Conductivity changes at 600 °C in dry 5% H_2/Ar of $Ce_{1-x}Ca_xVO_4$ with $0 \leq x \leq 0.4$

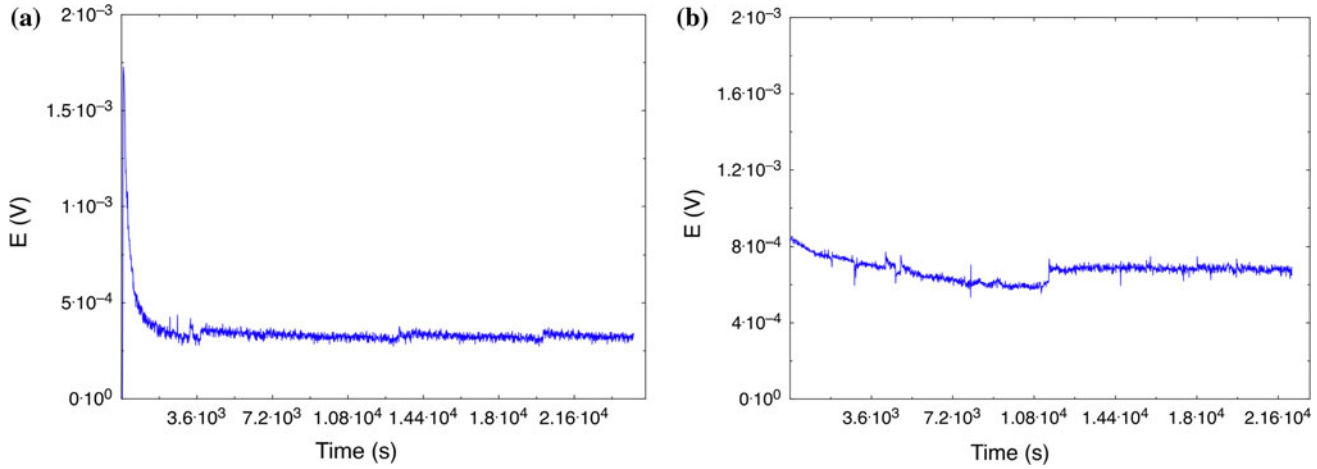

Fig. 11 OCV plots of $Ce_{0.7}Ca_{0.3}VO_4$ at 600 °C in 5% H_2/Ar–air electrochemical cell after 10 h (**a**) and 18 h (**b**), respectively

H_2/Ar. While rather small (0.38 mV after 10 h and 0.65 mV after 18 h), OCV values of the H_2/air electrochemical cell do indicate some ionic conduction, even if the electronic contribution is strongly dominating as under the aforementioned conditions an OCV of ~1.0 V would be expected for a pure ionic conducting electrolyte.

Some samples within the solid solution limit are redox stable during the conductivity measurement in 5% H_2/Ar up to 600 °C. As shown in Fig. 12, XRD pattern of samples $Ce_{0.9}Ca_{0.1}VO_4$ and $Ce_{0.8}Ca_{0.2}VO_4$ is almost unchanged upon reduction and can be considered as being redox stable below 600 °C. The marked peaks are metallic platinum reflections corresponding to the coating agent that could not be removed from the pellets and was therefore grinded with. For $x > 0.2$, samples were found to be relatively stable to reduced atmosphere treatment with CeO_2 traces detectable as a result of reducing oxygen pressure; process most likely due to traces of CeO_2 present in the product as impurity and intensified by treatment in H_2 atmosphere. The lattice expansion observed for samples with $x < 0.2$ on reduction is believed to be due to the reduction of both cerium and vanadium ions because both the Ce–O and the V–O bond lengths increased in the reduced sample. The bond lengths extracted from the pattern are—for $Ce_{0.8}Ca_{0.2}VO_4$ as an example—2.4780 Å for Ce–O (average) and 1.7074 Å for V–O when compared with 2.4595 Å for Ce–O (average) and 1.6949 Å for V–O before the conductivity measurement. Reversible change in conduction mechanism was observed for all compounds except for sample $Ce_{0.6}Ca_{0.4}VO_4$ at temperature ~575 °C resulting in an observed metallic behaviour during conductivity measurements (Fig. 13). Concerning activation energies in reduced atmosphere, values found were lower at low temperatures and higher at high temperatures than in air. Comparatively, while all activation energies in air for doped compounds were lower than for $CeVO_4$; in reduced atmosphere, either at high or low temperatures, $CeVO_4$ constants were lower than all others in accordance with conductivity variations.

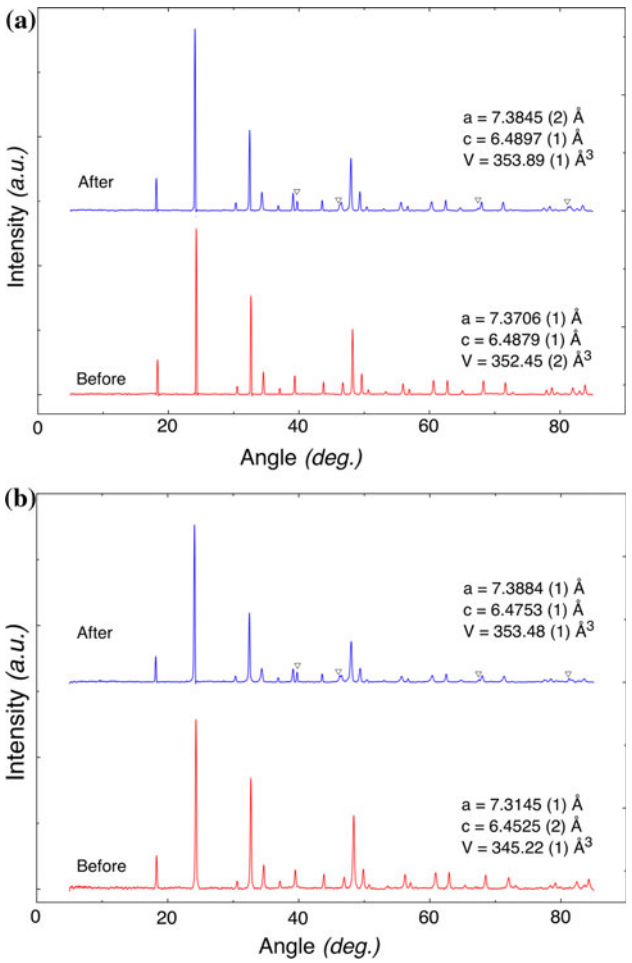

Fig. 12 X-ray diffraction pattern of **a** $Ce_{0.9}Ca_{0.1}VO_4$ and **b** $Ce_{0.8}Ca_{0.2}VO_4$ before and after conductivity measurement in dry 5% H_2/Ar. ∇—Metallic Pt

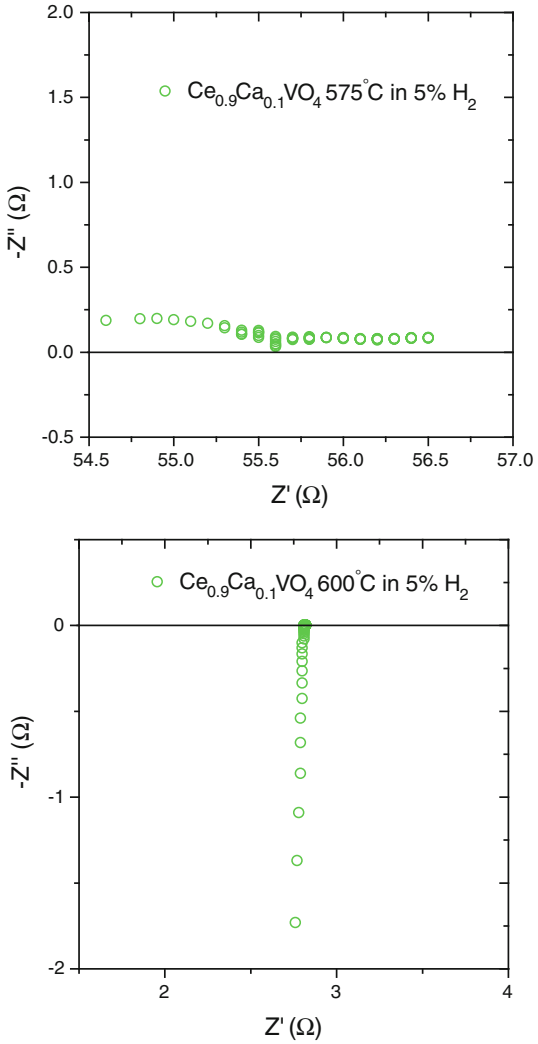

Fig. 13 Conductivity measurement plots of $Ce_{0.9}Ca_{0.1}VO_4$ at 600 and 575 °C in 5% H_2/Ar

Conclusion

Single-phase powders of $Ce_{1-x}Ca_xVO_4$ with $0 \leq x \leq 0.4125$ were synthesised by a standard ceramic technique. All samples were found to exhibit the tetragonal zircon-type structure of space group $I4_1/amd$. At room temperature, the solid solution limit in $Ce_{1-x}Ca_xVO_4$ series is at $x = 0.4125$. It is believed that the lattice contraction on Ca-doping is due to the change of charge of cerium ions from Ce^{3+} to Ce^{4+}. Conductivity measurements carried out in air and in reduced atmosphere have shown that the improvement in conductivity resulting from the doping is independent of the dopant level as well as of the temperature for the case of air, while $CeVO_4$ exhibits an increased conductivity in reduced atmosphere, doped species total conductivity is decreasing except for sample $Ce_{0.7}Ca_{0.3}VO_4$. The relatively lower conductivity in a reducing atmosphere will restrain the application of these materials as anode for intermediate temperature solid oxide fuel cells. Samples $Ce_{0.8}Ca_{0.2}VO_4$ and $Ce_{0.9}Ca_{0.1}VO_4$ are redox stable at a temperature below 600 °C although some lattice expansion was observed which is related to the reduction of both cerium and vanadium ions. The H_2/air electrochemical cell measurement indicates that the conduction of sample $Ce_{0.7}Ca_{0.3}VO_4$ is electronic dominant.

Acknowledgements The authors thank EPSRC for funding and Ms Marian Millar for the powder XRD data collection.

References

1. Milligan WO, Vernon LW (1952) J Phys Chem 56:145
2. Carron MK, Mrose ME, Murata K (1958) J Am Miner 43:985
3. Fuess H, Kallel A (1972) J Solid State Chem 5:11
4. Rice CE, Robinson WR (1976) Acta Crystallogr B 32:2232
5. Chakoumakos BC, Abraham MM, Boatner LA (1994) J Solid State Chem 109:197
6. CrystalMaker®, A crystal and molecular structures program for Mac and Windows, 1994-2009, CrystalMaker Software Ltd, Oxford, England. www.crystalmaker.com
7. Stencel JM (1990) in Raman Spectroscopy for Catalysts. Van Nostrand Reinhold, New York
8. Mahapatra S, Vinu R, Saha D, Guru Row TN, Madras G (2009) Appl Catal A 361:32
9. Milligan WO, Watt LM, Rachford HH (1949) J Phys Colloid Chem 53:227
10. Rao IS, Palanna OG (1995) Bull Mater Sci 18:593
11. Varma S, Wani BN, Gupta NM (2002) Mater Res Bull 37:2117
12. Watanabe A (2000) J Solid State Chem 153:174
13. Hirata T, Watanabe A (2001) J Solid State Chem 158:264
14. Tsipis EV, Kharton VV, Frade JR (2005) J Eur Ceram Soc 25:2623
15. Tsipis EV, Kharton VV, Frade JR, Vyshatko NP, Shaula AL (2003) J Solid State Chem 176:47
16. Tsipis EV, Patrakeev MV, Kharton VV, Vyshatko NP, Frade JR (2002) J Mater Chem 12:3738
17. Varma S, Wani BN, Gupta NM (2003) Appl Catal A 241:341
18. Varma S, Wani BN, Sathyamoorthy A, Gupta NM (2004) J Phys Chem Solids 65:1291
19. Larson AC, Von Dreele RB (2004) General structure analysis system (GSAS). Los Alamos National Laboratory Report, LAUR, 86. Los Alamos National Laboratory, New Mexico
20. Shannon RD (1976) Acta Cryst A 32:751
21. Petit CTG, Lan R, Cowin PI, Tao SW (2010) J Solid State Chem 183:1231
22. Tsipis EV, Munnings CN, Kharton VV, Skinner SJ, Frade JR (2006) Solid State Ion 177:1015